PPPL-2057

UC20-A,F

PPPL-2057

GAS FUELING STUDIES IN THE PDX TOKAMAK: II

By

H.F. Dylla, M.G. Bell, R.J. Fonck, K. Jaehnig, S.M. Kaye,
D.K. Owens, D.B. Heifetz, and G.L. Schmidt

JANUARY 1984

MASTER

PLASMA
PHYSICS
LABORATORY

PRINCETON UNIVERSITY
PRINCETON, NEW JERSEY

PREPARED FOR THE U.S. DEPARTMENT OF ENERGY,
UNDER CONTRACT DE-AC02-76-CHO-3073.

Gas Fueling Studies in the PDX Tokamak: II

H. F. Dylla, M. G. Bell, R. J. Fonck, K. Jaehnig, S. M. Kaye,
D. K. Owens, D. B. Heifetz, and G. L. Schmidt
Princeton Plasma Physics Laboratory, Princeton, N.J. 08544

ABSTRACT

Measurements of the gas fueling characteristics of the PDX tokamak have been extended in parameter range. An earlier study presented the gas fueling efficiency for H_2 and D_2 for the standard PDX divertor configurations with a large conductance between the divertor and main plasma chambers. This study presents the observed variations in H_2, D_2, and He neutral pressure and ionization light emission for divertor configurations with a restricted conductance between the divertor and main plasma chambers. The restricted conductance improved the divertor/main-chamber compression ratio by more than an order of magnitude. For the same plasma density, gas fueling from the divertor chamber was twice as efficient as fueling from the main chamber. At the highest plasma densities that were investigated, $\bar{n}_e = 4 \times 10^{13}$ cm^{-3}, a decrease in the plasma temperature in the divertor was indicated by a decrease in the ionization light at the divertor throat for D_2 and He fueled discharges. These observations are consistent with a Monte-Carlo model of neutral gas transport in the divertor.

Submitted to:
Symposium on Energy Removal and
Particle Control in Toroidal Fusion Devices
Princeton, New Jersey USA
26-29 July 1983

I. Introduction

In a previous study[1] of the gas fueling of ohmically heated discharges in the PDX tokamak, the fueling characteristics of a number of different divertor and limiter configurations were discussed. This paper focusses on the behavior of a divertor configuration in PDX with a more restricted conductance between the divertor and main plasma chambers. As a result of modifying the geometry, increased neutral pressure compression ratios between the divertor and main plasma chambers could be sustained, and transitions to "H-type"[2] plasmas were readily produced by neutral beam injection[3]. Although transitions into the H-regime did occur in plasmas with low compression ratios, only those discharges with high (10-20) compression ratios exhibited a significant improvement in confinement. The relationship between the change in divertor geometry and the appearance of the H-regime in PDX divertor discharges may not be causal. Nevertheless, the measurable effects of this change are important to document since a high compression ratio is a common factor in the divertor configurations which have demonstrated the H-regime in ASDEX[4], Doublet-III[5], and PDX[3].

In this paper, the fueling characteristics of the closed divertor configuration deduced from measurements of neutral pressures, gas influx, and ionization light emission are described. Comparisons were made between H_2, D_2, and He fueling with gas injection from the plasma midplane and from the divertor chamber. The measured neutral pressures and ionization light emission were compared with the predictions of a Monte-Carlo model of neutral transport in the divertor[6,7].

II. Experimental Considerations

The primary type of discharge investigated was a single-null, diverted plasma formed by displacing the PDX "dee" shaped plasma vertically upward by 4-5 cm. The plasma major radius was R = 140 cm, minor radius a = 40 cm, and plasma current range was typically I_p = 250-480 kA. These studies were limited to ohmically-heated plasmas, with a density range of $\bar{n}_e$ = $(1-4) \times 10^{13}$ cm^{-3}, that served as target plasmas for neutral beam heating experiments. Figure 1 shows the differences in the configuration of the vacuum vessel internal hardware between the "open" divertor geometry, which existed prior to November 1982, and the "closed" divertor geometry, which was in place after this date. This modification essentially blocked the channel for neutral gas that existed between the outer divertor lobe and the vessel wall. Additional modifications to the divertor shields were made in December 1982 to restrict further the conductance by blocking a number of diagnostic access holes in these shields. The remaining connection between the divertor and main chambers was essentially limited to the inner throats (with width ≈ 10 cm). For the majority of the discharges investigated, only the lower divertor chamber was gettered resulting in vessel pumping speeds for H_2 of ~ 50-100 kℓ/s.

For discussion of the measurements presented in the next section, it is important to point out the location of the instrumentation that was used in this study. High accuracy pressure measurements were made with magnetically-shielded fast ion gauges located on the plasma midplane and in the upper divertor chamber. The absolute calibration of these gauges is estimated to be ± 20%, and relative measurements can be made to ± 5%. For quantitative fueling studies, the gas influx rate was measured by monitoring the pressure drop in a calibrated volume located in the supply lines of the injection valves.

Ionization light emission from H_α, D_α, or HeII transitions was monitored by photomultipliers with appropriate interference filters that were located with line-of-sight view of (1) the plasma midplane at a location removed toroidally from the gas input, (2) the upper divertor throat, and (3) the upper divertor neutralizer plate.

III. Results

Figure 2 presents the neutral pressure measurements for the single-null divertor configuration with the closed geometry. The neutral pressure measured at the two locations, the upper divertor chamber and the plasma midplane, is plotted as a function f line-averaged plasma density, $\bar{n}_e$, with either H_2 or D_2 fueling injected at the midplane or in the divertor.

All the pressure curves shown in Fig. 2 exhibit a roughly exponential dependence with $\bar{n}_e$. At the highest densities that were investigated $\bar{n}_e$ = (3-4) x 10^{13} cm^{-3}, departures from a simple exponential fit are noted for both the H_2 and D_2 pressure curves. At high density the D_2 pressure shows a tendency to saturate for both midplane and divertor chamber pressures.

We define the compression ratio, C, as the ratio, P_D/P_M, of the pressure in the divertor chamber, P_D, to the pressure in the main plasma chamber, P_M. The previous open divertor geometry was unable to sustain a significant difference between P_D and P_M. The compression ratio was of the order of unity for this configuration for both H_2 and D_2 fueling, over a wide range of gas influx rates (1-200 Torr ℓ/s). However, only midplane gas injection was investigated with the open divertor.

The closed divertor geometry, in contrast, can sustain a significant compression ratio. Table 1 summarizes the achieved compression ratios in the four cases shown in Fig. 2. Note that since the midplane pressure curves are similar for all cases, the differences in C are the result of differences in divertor chamber pressure.

The data show that C can be doubled (from 10 to 20) by injecting the gas into the divertor chamber instead of the usual midplane location. The value of C could be lowered by gettering in the divertor chamber. For example, only moderate compression ratios (C = 3) were measured in the lower divertor which was gettered. In the case of H_2, the isolation of the divertor from the main chamber can be compromised by excessive gas feed, presumably through too large a neutral or plasma ion flow through the divertor, and the compression ratio collapses. This situation, termed a "blow-through" in the PDX literature[3], is identified by a large rise in midplane neutral pressure and a concurrent rise in midplane H_α emission.

No significant difference in neutral pressure distribution is evident between H_2 and D_2 fueling, except for a slightly larger compression ratio for D_2 in the case of midplane fueling. Figure 3 shows the only pressure curves which were obtained with He. Even with gas injection in the divertor chamber, only a moderate compression ratio of 5 is sustained with He.

The fueling efficiency of the closed geometry relative to the previously investigated open geometry[1] was studied by measuring the gas flow required to maintain a constant plasma density (Fig. 4). Fueling with H_2 injected into the divertor chamber in the closed geometry was found to have the same efficiency as fueling from the midplane with the open geometry, whereas, in the comparison of the two injection locations in the closed geometry, midplane fueling was found to require approximately twice as much gas as divertor fueling.

The behavior of the ionization light emission over the same density range as the pressure measurements is shown in Fig. 5 (for D_α emission) and Fig. 6 (for HeII emission). At the highest densities $n_e > 3 \times 10^{13}$ cm^{-3} a saturation or even a decrease in D_α (or HeII) emission is noted for the measurements in the divertor.

IV. Discussion

The closed divertor geometry allowed a significant neutral pressure difference to be sustained between the edge plasma region at the plasma midplane and divertor chamber. Not surprisingly, the compression ratios (P_D/P_M) could be increased by injecting gas directly into the divertor chamber or by applying less divertor pumping. The measured compression ratios are in good agreement with the predictions of a numerical model of the PDX divertor using the neutral transport code DEGAS[6].

We have analyzed the set of data which is most complete, the case of divertor fueling with D_2, by combining a simplified model of H_α emission[8], with the DEGAS code.

For the electron density and temperature (T_e) ranges expected in the divertor, the H_α light emission (Γ) varies approximately as

$$\Gamma \simeq K \cdot n_e n_o T_e^{\alpha}, \text{ where } \alpha = \begin{cases} 5.3, & T_e < 5 \text{ eV} \\ 1.0, & 5 < T_e < 60 \text{ eV}, \end{cases}$$

where n_o is the density of atomic hydrogen, and K is a constant. Assuming n_o is proportional to neutral pressure, T_e can be computed from the data shown in Figs. 2d, 5, and from the measured divertor density shown in Fig. 7. The predicted dependence of T_e on $\bar{n}_e$ is shown in Fig. 8. The curve has been scaled at one point to an experimental value of T_e = 15 eV at $\bar{n}_e = 2.5 \times 10^{13}$ cm^{-3} that was measured with a Langmuir probe positioned on the separatrix in the divertor[9]. The predicted value of T_e is found to decrease from 60-70 eV at $\bar{n}_e = 1 \times 10^{13}$ cm^{-3} to 6-8 eV at $\bar{n}_e = 3 \times 10^{13}$ cm^{-3}. Above $\bar{n}_e = 3 \times 10^{13}$ cm^{-3}, T_e drops below 5 eV, and so, as Γ varies as $T_e^{5.3}$, the rate of fall in T_e is smaller, T_e dropping to 4-5 eV at $\bar{n}_e = 4 \times 10^{13}$ cm^{-3}. A second experimental measurement of T_e (at $\bar{n}_e \approx 4 \times 10^{13}$ cm^{-3}), which is an upper limit inferred from the threshold of OII (4415Å) emission[10], confirms that divertor plasma cools at high densities.

Using the measured $\bar{n}_e$ and the T_e computed above (from the measured $\bar{n}_e$, H_α emission, and neutral pressure), neutral transport was computed using the code DEGAS, with the same geometry, physical assumptions, and limitations described in [7]. The calculated neutral pressures and H_α emission are shown with the respective experimental data in Figs. 2d and 5. The computed neutral pressure agrees well with the measured pressure when a flow velocity Mach number of 0.11 is used. The calculated H_α emission agrees qualitatively with the density dependence of the measured emission at the throat. (No attempt was made at a quantitative comparison of absolute intensities.) With this agreement our model appears to give a self-consistent picture of n_e, n_o, and T_e in the divertor.

The comparison of divertor plate power measurements[11] also shows good agreement with our model, except at the lowest density ($\bar{n}_e \sim 1 \times 10^{13}$). Here the experimental data indicates a lower electron temperature of about 45 eV.

The cooling of T_e to under 5 eV for $\bar{n}_e$ above 3×10^{13} cm^{-3}, which was derived from the H_α emission, results in the probability of electron impact ionization becoming negligible in comparison to charge exchange. This high density, low temperature regime of operation for a divertor has been predicted by previous modeling studies[12], and it has also been observed in ASDEX[4]. The calculated re-ionization probability of neutrals (Fig. 8), decreases from 0.85 at $\bar{n}_e = 1 \times 10^{13}$ cm^{-3} to 0.50 at $\bar{n}_e = 4 \times 10^{13}$ cm^{-3}. Thus, the colder plasma is more transparent to the neutrals, reducing the ability of the divertor to maintain neutral pressure. This explanation is consistent with the saturation observed in the D_2 pressure curve as $\bar{n}_e$ rises above 3×10^{13} cm^{-3} (Fig. 3d).

The behavior of the electron temperature at high densities may also explain the collapse in compression seen during high flow gas fueling (blow-through). The drop in ionization probability with lowered T_e results in a lower fueling efficiency at the higher densities; thus more neutral gas can stream through the divertor raising the midplane neutral pressure.

Figure Captions

Fig. 1 (a) Diagram of the standard "dee" divertor configuration in PDX that was the primary divertor discharge configuration investigated prior to November 1982.

(b) Diagram of the single-null divertor configuration used after November 1982 with baffling installed between the divertor and main plasma chambers to restrict the conductance.

Fig. 2 Neutral pressure measured in the upper divertor chamber and main plasma chamber as a function of line-averaged plasma density for (a) H_2 midplane fueling; (b) H_2 divertor fueling; (c) D_2 midplane fueling; and (d) D_2 divertor fueling.

Fig. 3 Neutral pressure as a function of line-averaged plasma density for He fueling from the divertor.

Fig. 4 Comparison of the H_2 flow required to maintain a constant plasma density.

Fig. 5 Variation of the D_α emission as a function of line-averaged plasma density.

Fig. 6 Variation of the HeII emission as a function of the line-averaged plasma density.

Fig. 7 Measured line-averaged plasma density in the divertor throat as a function of the main chamber line-averaged density.

Fig. 8 Calculated electron temperature (T_e) in the divertor as a function of the line-averaged plasma density in the main chamber. Also shown are experimental measurements of T_e inferred from a Langmuir probe measurement (P) and OII emission (O). The inset shows the calculated ionization probability for an ion neutralized at the divertor plate to reionize in the divertor. The corresponding probability for ionization of a molecule injected into the divertor is essentially the same.

Table 1: Compression Ratios in PDX Diverted Discharges

Divertor Configuration	H_2	D_2	He
Open:	1-2	1-2	—
Closed:			
midplane gas feed	10	12	—
dome gas feed	20	20	5

References

[1] H. F. Dylla *et al.*, J. Nucl. Mater. 111 & 112, 211 (1982).

[2] F. Wagner *et al.*, Phys. Rev. Lett. 49, 1408 (1982).

[3] S. M. Kaye *et al.*, in Proceedings on Energy Removal and Particle Control in Toroidal Fusion Devices, Princeton, NJ, July 26-29, 1983.

[4] M. Keilhacker *et al.*, in Proceedings on Energy Removal and Particle Control in Toroidal Fusion Devices, Princeton, NJ, July 26-29, 1983.

[5] N. Ohyaba *et al.*, in Proc. IEEE Intern. Conf. on Plasma Science (San Diego, CA, May 1983).

[6] D. B. Heifetz *et al.*, J. Comp. Phys. 46 (1982) 309.

[7] D. B. Heifetz, *et al.*, in Proceedings on Energy Removal and Particle Control in Toroidal Fusion Devices, Princeton, NJ, July 26-29, 1983.

[8] J. Weisheit, J. Phys. B: Atom. Molec. Phys., 8 (1975) 2556.

[9] D. K. Owens and S. M. Kaye, in Proceedings on Energy Removal and Particle Control in Toroidal Fusion Devices, Princeton, NJ, July 26-29, 1983.

[10] Concurrent with the decrease in D_α intensity, the intensity of the OII 4415Å line emission from the divertor dropped by a factor of four or more when $\bar{n}_e$ was increased from 3×10^{13} cm^{-3} to 4×10^{13} cm^{-3}. Assuming that the source of neutral oxygen in the divertor region did not decrease as $\bar{n}_e$ increased, this drop in OII emission is consistent with a decrease in T_e in the divertor from 15 eV at $\bar{n}_e = 2 \times 10^{13}$ cm^{-3} (as measured by the Langmuir probe) to less than 10 eV at $\bar{n}_e$ = 4×10^{13} cm^{-3}.

[11] M. Bell *et al.*, in Proceedings on Energy Removal and Particle Control in Toroidal Fusion Devices, Princeton, NJ, July 26-29.

[12] M. Petravic *et al.*, Phys. Rev. Lett *48*, 326 (1982).

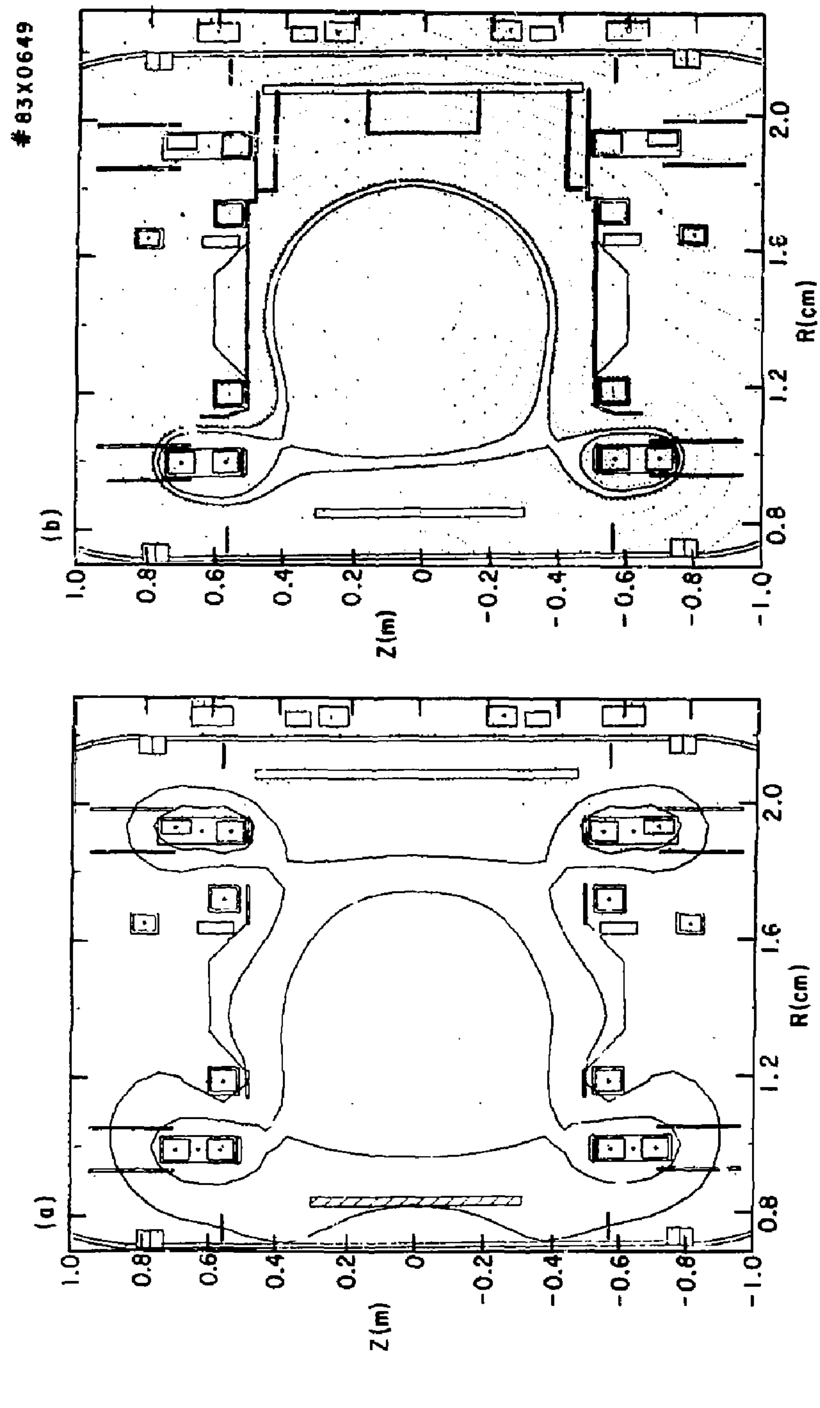

Fig. 1

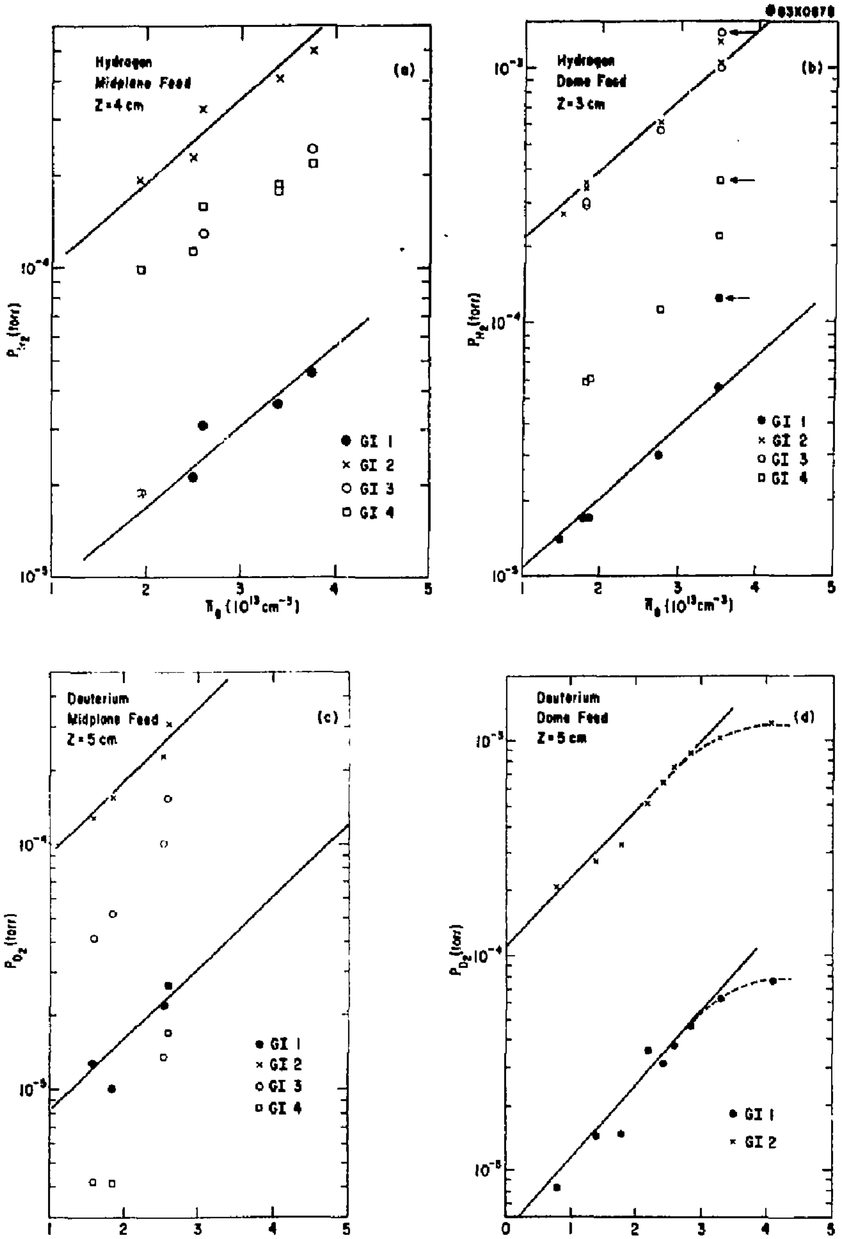
Hydrogen
Midplane Feed
Z=4 cm
(a)
GI 1
GI 2
GI 3
GI 4
Hydrogen
Dome Feed
Z=3 cm
(b)
GI 1
GI 2
GI 3
GI 4
Deuterium
Midplane Feed
Z=5 cm
(c)
GI 1
GI 2
GI 3
GI 4
Deuterium
Dome Feed
Z=5 cm
(d)
GI 1
GI 2

Fig. 2

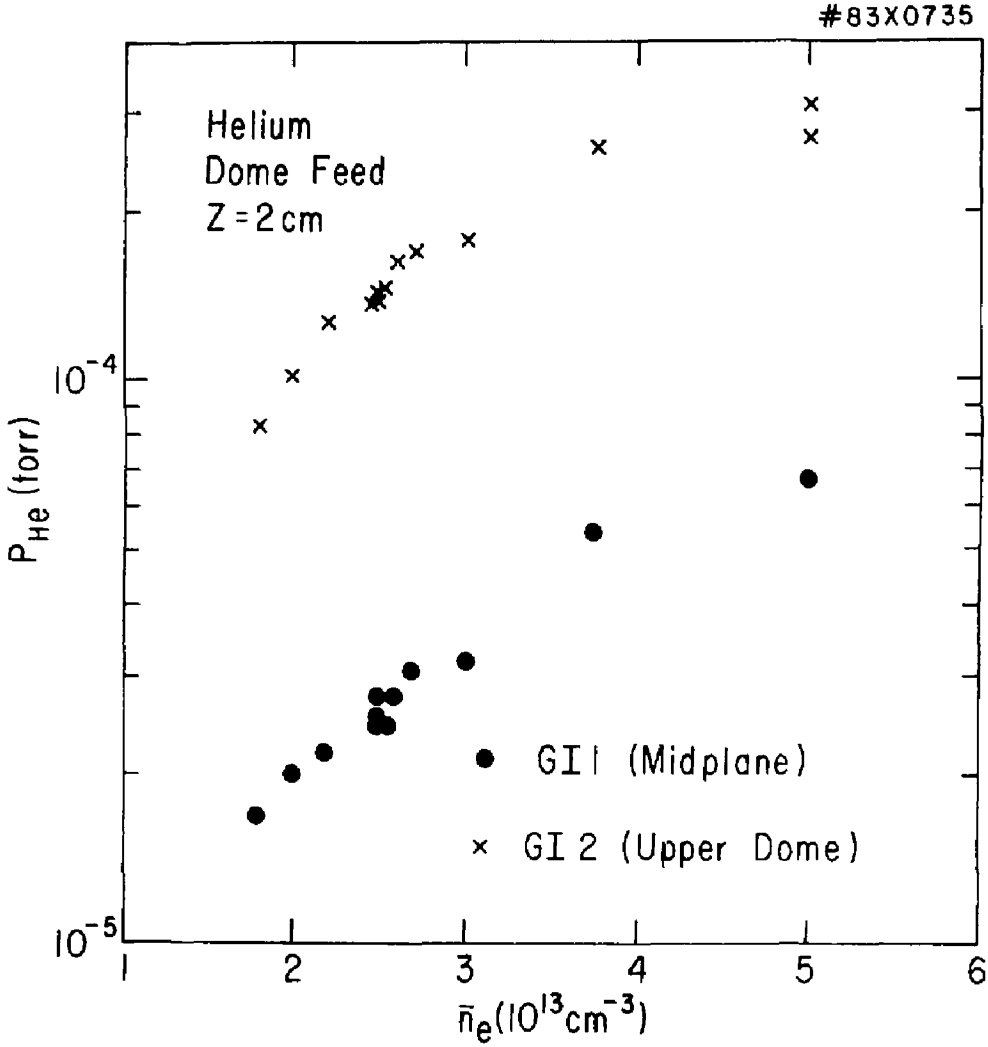
#83X0735
Helium
Dome Feed
Z = 2 cm
GI 1 (Midplane)
GI 2 (Upper Dome)
P_{He} (torr)
10^{-4}
10^{-5}
1
2
3
4
5
6
$\bar{n}_e(10^{13}cm^{-3})$

Fig. 3

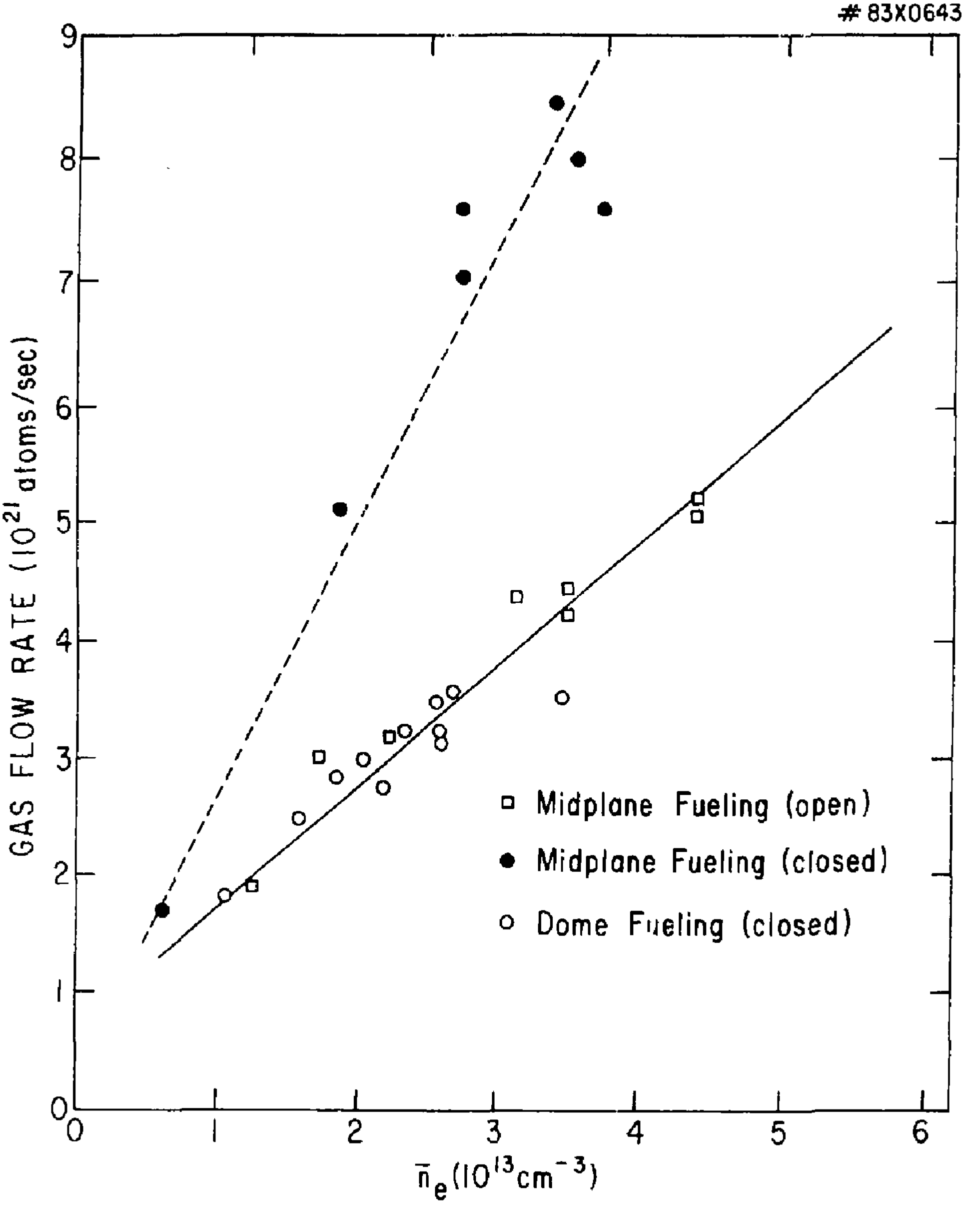
#83X0643
GAS FLOW RATE (10^{21} atoms/sec)
$\bar{n}_e$ (10^{13} cm^{-3})
Midplane Fueling (open)
Midplane Fueling (closed)
Dome Fueling (closed)
0
1
2
3
4
5
6
7
8
9
0
1
2
3
4
5
6

Fig. 4

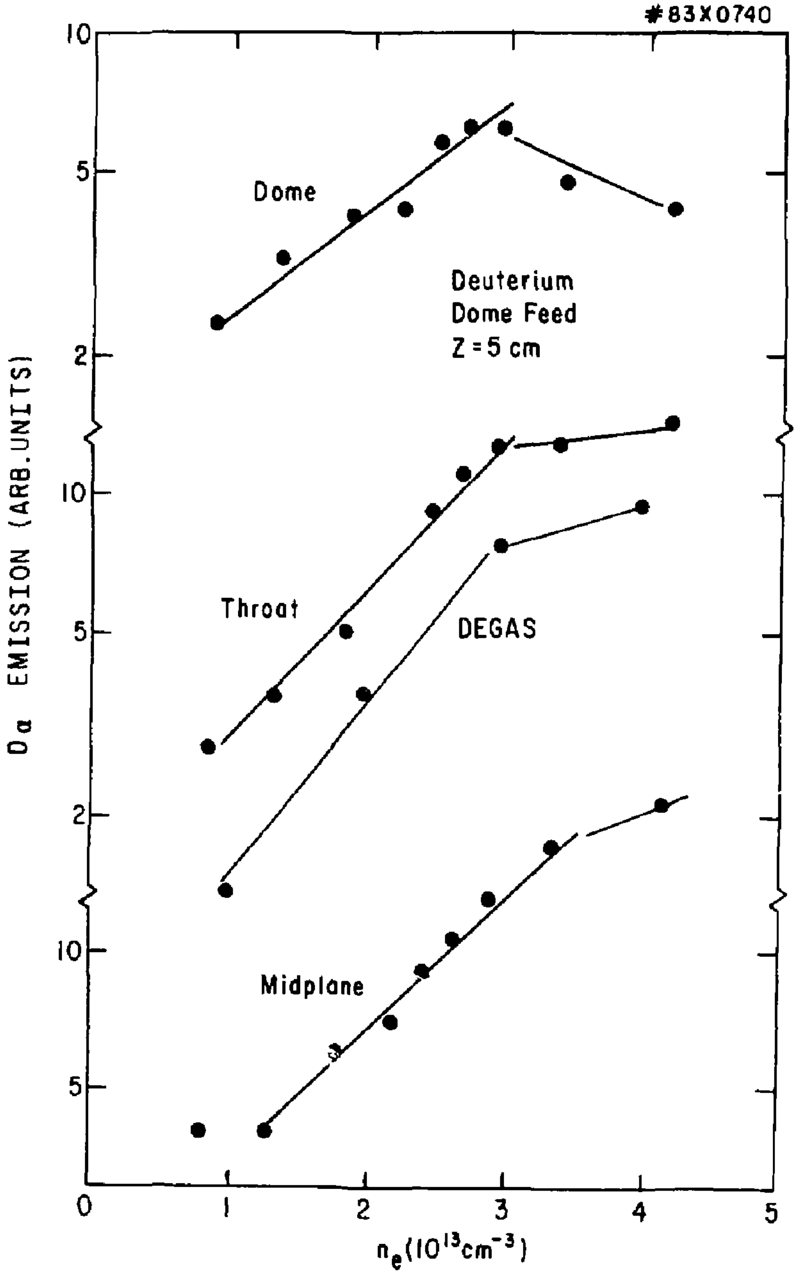
#83X0740
Dome
Deuterium
Dome Feed
Z = 5 cm
Throat
DEGAS
Midplane
Dα EMISSION (ARB. UNITS)
10
5
2
10
5
2
10
5
0
1
2
3
4
5
$n_e(10^{13}cm^{-3})$

Fig. 5

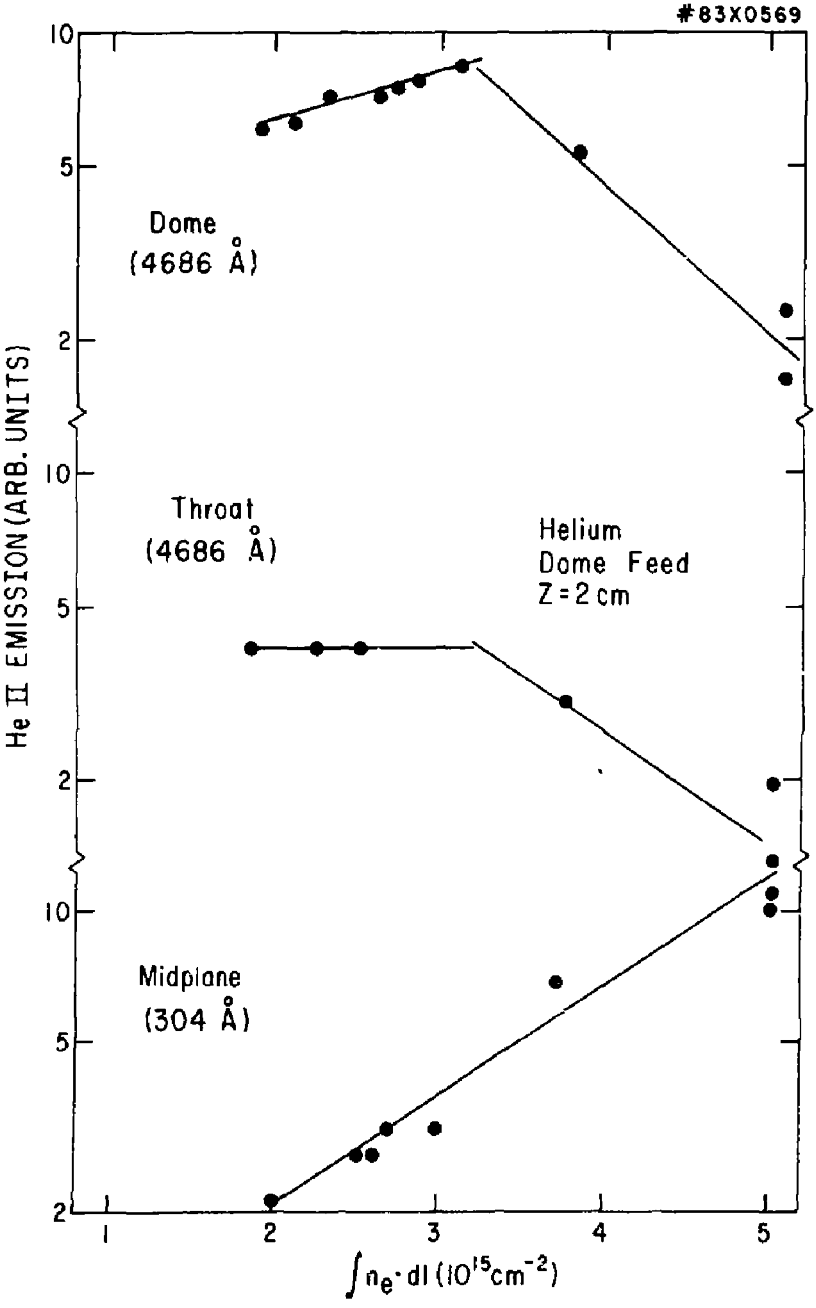
#83X0569
He II EMISSION (ARB. UNITS)
Dome
(4686 Å)
Throat
(4686 Å)
Helium
Dome Feed
Z = 2 cm
Midplane
(304 Å)
$\int n_e \cdot dl\ (10^{15} cm^{-2})$
10
5
2
10
5
2
10
5
2
1
2
3
4
5

Fig. 6

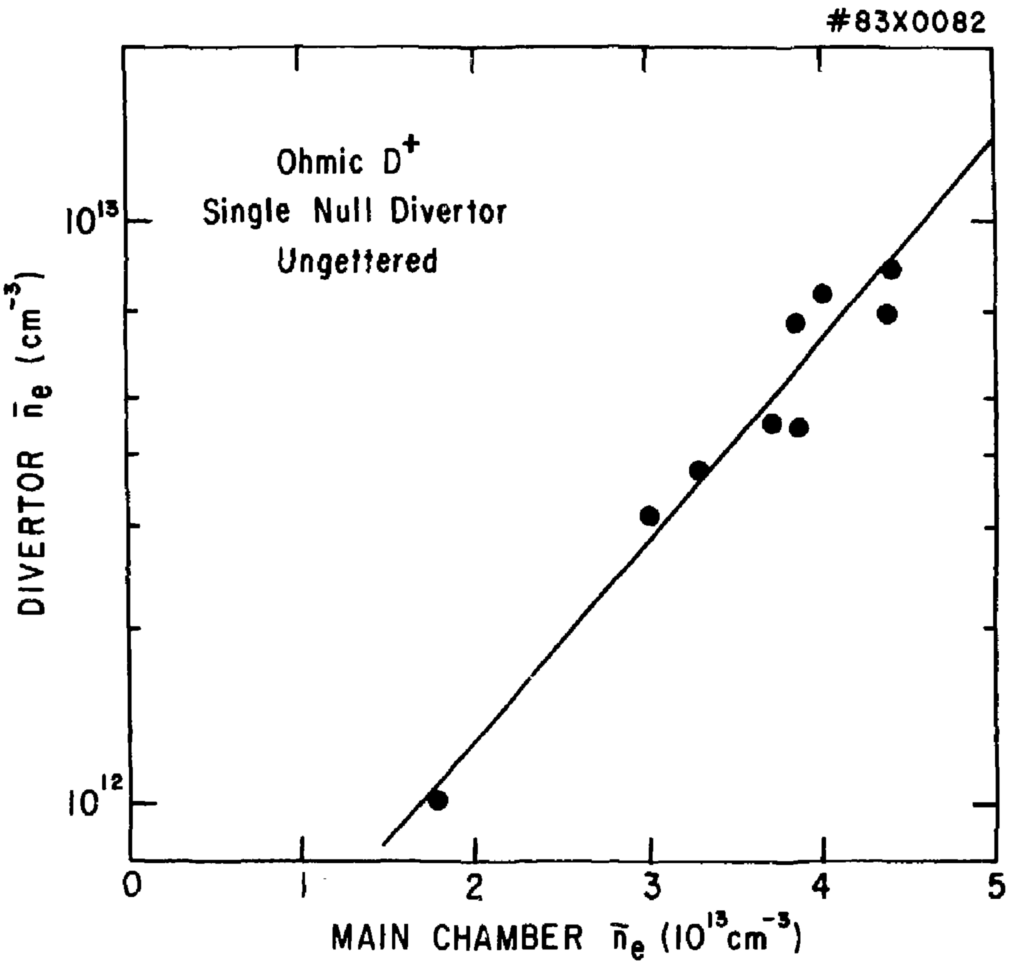
#83X0082
Ohmic D+
Single Null Divertor
Ungettered
10^13
10^12
DIVERTOR n̄e (cm^-3)
0
1
2
3
4
5
MAIN CHAMBER n̄e (10^13 cm^-3)

Fig. 7

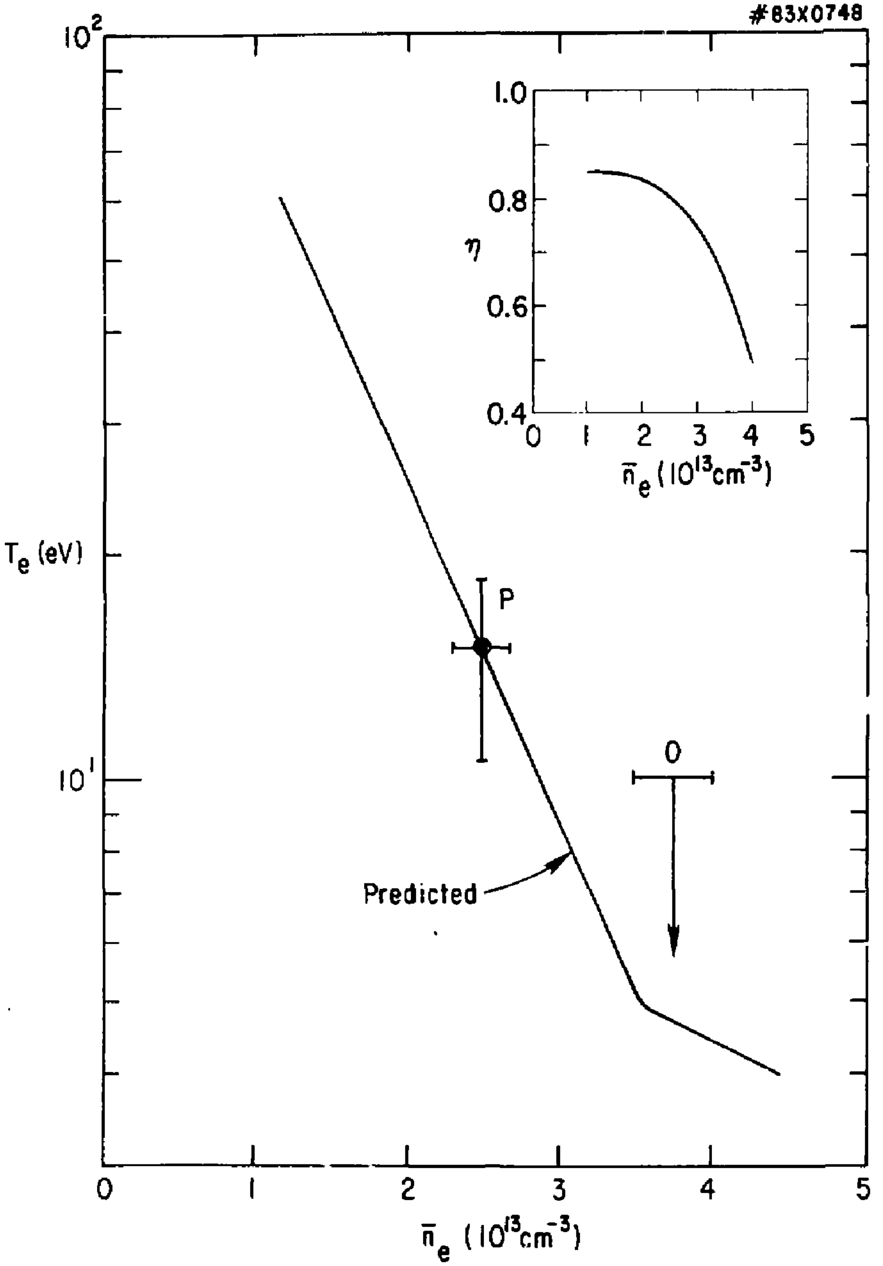
#83X0748
10^2
10^1
T_e (eV)
1.0
0.8
0.6
0.4
η
0
1
2
3
4
5
$\bar{n}_e$ (10^{13}cm^{-3})
P
O
Predicted
0
1
2
3
4
5
$\bar{n}_e$ (10^{13}cm^{-3})

Fig. 8

EXTERNAL DISTRIBUTION IN ADDITION TO TIC UC-20

Plasma Res Lab, Austra Nat'l Univ, AUSTRALIA
Dr. Frank J. Paoloni, Univ of Wollongong, AUSTRALIA
Prof. I.R. Jones, Flinders Univ., AUSTRALIA
Prof. M.H. Brennan, Univ Sydney, AUSTRALIA
Prof. F. Cap, Inst Theo Phys, AUSTRIA
Prof. Frank Verheest, Inst theoretische, BELGIUM
Dr. D. Palumbo, Dg XII Fusion Prog, BELGIUM
Ecole Royale Militaire, Lab de Phys Plasmas, BELGIUM
Dr. P.H. Sakanaka, Univ Estadual, BRAZIL
Dr. C.R. James, Univ of Alberta, CANADA
Prof. J. Teichmann, Univ of Montreal, CANADA
Dr. H.M. Skarsgard, Univ of Saskatchewan, CANADA
Prof. S.R. Sreenivasan, University of Calgary, CANADA
Prof. Tudor W. Johnston, INRS-Energie, CANADA
Dr. Hannes Barnard, Univ British Columbia, CANADA
Dr. M.P. Bachynski, MPB Technologies, Inc., CANADA
Zhengwu Li, SW Inst Physics, CHINA
Library, Tsing Hua University, CHINA
Librarian, Institute of Physics, CHINA
Inst Plasma Phys, Academia Sinica, CHINA
Dr. Peter Lukac, Komenskeho Univ, CZECHOSLOVAKIA
The Librarian, Culham Laboratory, ENGLAND
Prof. Schatzman, Observatoire de Nice, FRANCE
J. Radet, CEN-BP6, FRANCE
AM Dupas Library, AM Dupas Library, FRANCE
Dr. Tom Mual, Academy Bibliographic, HONG KONG
Preprint Library, Cent Res Inst Phys, HUNGARY
Dr. S.K. Trehan, Panjab University, INDIA
Dr. Indra, Mohan Lal Das, Banaras Hindu Univ, INDIA
Dr. L.K. Chavda, South Gujarat Univ, INDIA
Dr. R.K. Chhajlani, Var Ruchi Marg, INDIA
P. Kaw, Physical Research Lab, INDIA
Dr. Phillip Rosenau, Israel Inst Tech, ISRAEL
Prof. S. Cuperman, Tel Aviv University, ISRAEL
Prof. G. Rostagni, Univ Di Padova, ITALY
Librarian, Int'l Ctr Theo Phys, ITALY
Miss Clelia De Palo, Assoc EURATOM-CNEN, ITALY
Biblioteca, del CNR EURATOM, ITALY
Dr. H. Yamato, Toshiba Res & Dev, JAPAN
Prof. M. Yoshikawa, JAERI, Tokai Res Est, JAPAN
Prof. T. Uchida, University of Tokyo, JAPAN
Research Info Center, Nagoya University, JAPAN
Prof. Kyoji Nishikawa, Univ of Hiroshima, JAPAN
Prof. Sigeru Mori, JAERI, JAPAN
Library, Kyoto University, JAPAN
Prof. Ichiro Kawakami, Nihon Univ, JAPAN
Prof. Satoshi Itoh, Kyushu University, JAPAN
Tech Info Division, Korea Atomic Energy, KOREA
Dr. R. England, Civdad Universitaria, MEXICO
Bibliotheek, Fom-Inst Voor Plasma, NETHERLANDS
Prof. B.S. Liley, University of Waikato, NEW ZEALAND
Dr. Suresh C. Sharma, Univ of Calabar, NIGERIA
Prof. J.A.C. Cabral, Inst Superior Tech, PORTUGAL
Dr. Octavian Petrus, ALI CUZA University, ROMANIA
Prof. M.A. Hellberg, University of Natal, SO AFRICA
Dr. Johan de Villiers, Atomic Energy Bd, SO AFRICA
Fusion Div. Library, JEN, SPAIN
Prof. Hans Wilhelmson, Chalmers Univ Tech, SWEDEN
Dr. Lennart Stenflo, University of UMEA, SWEDEN
Library, Royal Inst Tech, SWEDEN
Dr. Erik T. Karlson, Uppsala Universitet, SWEDEN
Centre de Recherchesen, Ecole Polytech Fed, SWITZERLAND
Dr. W.L. Weise, Nat'l Bur Stand, USA
Dr. W.M. Stacey, Georg Inst Tech, USA
Dr. S.T. Wu, Univ Alabama, USA
Prof. Norman L. Oleson, Univ S Florida, USA
Dr. Benjamin Ma, Iowa State Univ, USA
Prof. Magne Kristiansen, Texas Tech Univ, USA
Dr. Raymond Askew, Auburn Univ, USA
Dr. V.T. Tolok, Kharkov Phys Tech Ins, USSR
Dr. D.D. Ryutov, Siberian Acad Sci, USSR
Dr. G.A. Eliseev, Kurchatov Institute, USSR
Dr. V.A. Glukhikh, Inst Electro-Physical, USSR
Institute Gen. Physics, USSR
Prof. T.J. Boyd, Univ College N Wales, WALES
Dr. K. Schindler, Ruhr Universitat, W. GERMANY
Nuclear Res Estab, Julich Ltd, W. GERMANY
Librarian, Max-Planck Institut, W. GERMANY
Dr. H.J. Kaeppler, University Stuttgart, W. GERMANY
Bibliothek, Inst Plasmaforschung, W. GERMANY